





Power quality improvement of smart microgrids using EMS-based fuzzy controlled UPQC

Ahmed HOSSAM-ELDIN¹, Ahmed MANSOUR^{1,*}, Mohamed ELGAMAL², Karim YOUSSEF¹

¹Department of Electrical Engineering, Faculty of Engineering, Alexandria University, Alexandria, Egypt

²Department of Operation Service, SUMED Company, Alexandria, Egypt

Received: 18.07.2018

Accepted/Published Online: 17.12.2018

Final Version: 22.03.2019

Abstract: The prevalent power quality problems in smart microgrids and power distribution systems are voltage sag, voltage swell, and harmonic distortion. The achievement of pure sinusoidal waveform with proper magnitude and phase is currently a great research and development concern. The aim of this paper is to evaluate and mitigate the smart microgrid harmonics, voltage sag, and voltage swell throughout a 24-h cycle, taking into consideration the variation in solar power generation due to changes in irradiation received by photovoltaic cells, the variation in wind power generation due to changes in wind speed, and the variation of linear and nonlinear load profiles during the day's cycle. The mitigation of the power quality issues manifested in current harmonics, voltage sag, and voltage swell is achieved through the implementation of a new fully fuzzy controlled unified power quality conditioner (UPQC). It is controlled by an energy management system (EMS). This paper introduces a new control system for the UPQC using full fuzzy logic control. Moreover, fuzzy control is used in current control instead of proportional integral controllers so that it has acceptable performance over a wide range of operating points. The novel approach of an EMS-connected UPQC activates the UPQC at the required time only into the grid. This approach has many benefits by increasing the UPQC lifetime. The effect of the proposed system on the aforementioned issues has been validated through simulation by MATLAB/Simulink. The results are compared with those obtained by conventional methods. The results verify the superior performance of the proposed UPQC to mitigate the problems of current total harmonic distortions, voltage sag, and voltage swell under different operating conditions during the monitoring period.

Key words: Smart microgrids, power quality, fuzzy logic control, harmonics, voltage sag, voltage swell, shunt active filter, series active filter, UPQC

1. Introduction

The smart grid is a concept and vision that captures a range of advanced information, sensing, communication, control, and energy technology [1]. The power quality challenges in smart microgrids are mainly described by the current harmonic limits set by IEEE 519. The percentage of total harmonic distortions (THDs) at the end-user should not exceed 5% [2]. Voltage sag is defined by IEEE 1159 as the decrease in the RMS voltage level to 10%–90% of the nominal value of the power frequency for a duration of half cycle to one minute [3]. Voltage swell is defined by IEEE 1159 as the increase in the RMS voltage level to 110%–180% of nominal at the power frequency for a duration of a half cycle to 1 min [3]. As per IEEE 1547, when the distributed resources are serving balanced linear loads, the percentage THD must not exceed the limit of 5% harmonic current [4]. The

*Correspondence: ahmed7315@hotmail.com

delivered power quality is the main concern for consumers, electrical generation and distribution companies, and researchers. Accordingly, this issue has been the subject of most recent works concerning smart microgrids. The commonly used standards and protocols in smart grids were introduced in [5]. Fang presented the connotations of both flexible AC transmission systems (FACTS) and resilient AC distribution systems (RACD) for a smart grid [6] and summarized the current efforts as the concepts of both FACTS and RACDS for a smart grid, different configurations, key benefits, operating principles, and world-wide installations of FACTS and RACDS devices. The existing power quality disturbances in traditional and smart grids were discussed in [7]. A technical discussion of microgrids and smart grids with current developments and future trends was presented in [8]. This review discussed the microgrid architecture and functions. In [8], smart features were added to the microgrid to demonstrate the recent architecture of smart grids. The expected power quality when introducing several smart distribution grid technologies and applications was mapped in [9], by discussing microgrids, advanced voltage control, feeder reconfiguration, and demand side management. The application of advanced power electronics in smart grids was studied in [10], with emphasis on the application of FACTS technology, high voltage DC current (HVDC) transmission system technology, and power quality technology in smart grids. Moayed et al. presented a new power device for real-time control of reactive power. Their approach takes advantage of the online smart meter data transmitted from each bus to the smart grid central control to concurrently perform the static synchronous compensator and active power line conditioner operations by optimal compensations of fundamental reactive power and harmonic currents at selected optimal buses [11]. A literature survey of FACTS technology tools and applications for power quality and efficient renewable energy system utilization was presented in [12]. In [13], a design of a hybrid AC/DC microgrid for optimization of the performance of a smart grid was introduced using a new UPQC named UPQC-DC to improve the power quality, control the power flow, compensate for reactive power, and control the power swing for the hybrid AC/DC microgrid system.

A study of the power quality constrained optimization of smart microgrids with nonlinear loads for multiple transitions to grid-connected and islanded modes was proposed by Karim [14], who focused on optimal management of nonlinear loads considering the harmonics limitations. However, he did not introduce any power filters for harmonics mitigation. Information and communication technology-based power control UPQC was presented in [15] to manage cooperation between series parts and shunt parts of open UPQC, but this work only focused on control and the information communication between open UPQC parts. The harmonic disturbances present in a real smart grid were assessed in [16]. The authors suggested a method to keep the operation of the distribution system with PV plant and electrical cars within power quality limits imposed by standards. However, they used passive power filters only. The impact of connecting renewable sources to smart grids regarding power quality was presented in [17], but the authors did not introduce any power filters for the mentioned power quality problem mitigation in their work. The design phases related to an open UPQC installed in a real low voltage distribution grid were discussed in [18]. However, this research introduced a new configuration of the open UPQC and did not introduce a clear contribution in UPQC power filter control.

Most of the literature on UPQC control adopted the use of PI controllers [19]. PI controller design is based on a linearized model about certain operating points only. The performance deteriorates if the operating points are changed. In most research papers, P-Q theory is used for reference control generation [19]. Some trials in the literature, as in [20, 21], used fuzzy logic control only in the UPQC shunt part. In this paper, a new simple fuzzy controlled UPQC using a completely fuzzy logic control system in both parts of the UPQC is

introduced. The new UPQC proposed design based on fuzzy control does not need an accurate mathematical model or P-Q calculation. The fuzzy controlled UPQC is proposed here to mitigate harmonics, voltage sag, and swell for the smart microgrid system during a 24-h cycle, considering the effect of variation of renewable energy and loads throughout the day's cycle. The control of activation duty of UPQC parts depending on need has not been investigated in previous publications. In this paper, the UPQC is fully controlled from the smart grid EMS. This new method activates the UPQC at the required time only. This paper is outlined as follows: in Section 2, the P-Q UPQC control system is introduced; in Section 3, the proposed complete fuzzy controlled UPQC is designed and implemented and the proposed control system between the EMS and UPQC is illustrated; in Section 4, the used system under study is introduced; in Section 5, the results of the proposed work are presented and discussed, and the results are compared with the traditional techniques; and in Section 6, the conclusion is discussed.

2. UPQC based on P-Q method

Basically, the UPQC is equipment used for power quality mitigation that compensates for current harmonic distortions, voltage sag, and voltage swell in the power system. The UPQC is a combination of a shunt active power filter (SHAF) and series active power filter (SEAF). The SHAF is used to compensate for nonlinear load current harmonics and makes the source current completely sinusoidal and free from harmonics. The SEAF is used to mitigate the voltage sag and voltage swell in the supply side and perfectly regulate the voltage at the load side.

The conventional P-Q method [22] is used to generate the SHAF reference currents. Three-phase voltages and currents are transformed from the (a, b, c) frame to the (α, β) frame using Clark's transformation as follows:

$$\begin{bmatrix} V_0 \\ V_\alpha \\ V_\beta \end{bmatrix} = \sqrt{\frac{2}{3}} \cdot \begin{bmatrix} \frac{1}{\sqrt{2}} & \frac{1}{\sqrt{2}} & \frac{1}{\sqrt{2}} \\ 1 & \frac{-1}{2} & \frac{-1}{2} \\ 0 & \frac{\sqrt{3}}{2} & -\frac{\sqrt{3}}{2} \end{bmatrix} \cdot \begin{bmatrix} V_a \\ V_b \\ V_c \end{bmatrix}, \quad (1)$$

$$\begin{bmatrix} i_0 \\ i_\alpha \\ i_\beta \end{bmatrix} = \sqrt{\frac{2}{3}} \cdot \begin{bmatrix} \frac{1}{\sqrt{2}} & \frac{1}{\sqrt{2}} & \frac{1}{\sqrt{2}} \\ 1 & \frac{-1}{2} & \frac{-1}{2} \\ 0 & \frac{\sqrt{3}}{2} & -\frac{\sqrt{3}}{2} \end{bmatrix} \cdot \begin{bmatrix} i_a \\ i_b \\ i_c \end{bmatrix}, \quad (2)$$

where v_α is the voltage in the (α) coordinate, v_β is the voltage in the (β) coordinate, V_0 is the fundamental zero sequence component of the line voltage, i_α is the current in the (α) coordinate, i_β is the current in the (β) coordinate, and i_0 is the fundamental zero sequence component of the line current.

The instantaneous active and reactive powers in the α, β coordinates are calculated with the following equations:

$$p(t) = v_\alpha(t) \cdot i_\alpha(t) + v_\beta(t) \cdot i_\beta(t), \quad (3)$$

$$q(t) = -v_\alpha(t) \cdot i_\beta(t) + v_\beta(t) \cdot i_\alpha(t), \quad (4)$$

$$\begin{bmatrix} i_\alpha \\ i_\beta \end{bmatrix} = \frac{1}{v_\alpha^2 + v_\beta^2} \cdot \left\{ \begin{bmatrix} v_\alpha & v_\beta \\ v_\beta & -v_\alpha \end{bmatrix} \cdot \begin{bmatrix} p \\ 0 \end{bmatrix} + \begin{bmatrix} v_\alpha & v_\beta \\ v_\beta & -v_\alpha \end{bmatrix} \cdot \begin{bmatrix} 0 \\ q \end{bmatrix} \right\} = \begin{bmatrix} i_{\alpha p} \\ i_{\beta p} \end{bmatrix} + \begin{bmatrix} i_{\alpha q} \\ i_{\beta q} \end{bmatrix}, \quad (5)$$

$$p = \bar{p} + \tilde{p}, \quad (6)$$

$$q = \bar{q} + \tilde{q}. \quad (7)$$

In order to compensate the reactive power and current harmonics generated by nonlinear loads, the reference signal of the SHAF must include the values corresponding to \tilde{p}_L , \bar{q}_L , and \tilde{q}_L . Harmonic active power is extracted using a second-order filter and then the reference currents of the SHAF are calculated as follows:

$$\begin{bmatrix} i_{c,\alpha}^* \\ i_{c,\beta}^* \end{bmatrix} = \frac{1}{v_\alpha^2 + v_\beta^2} \cdot \begin{bmatrix} v_\alpha & v_\beta \\ v_\beta & -v_\alpha \end{bmatrix} \cdot \begin{bmatrix} \tilde{p}_L \\ \bar{q}_L + \tilde{q}_L \end{bmatrix}, \quad (8)$$

$$\begin{bmatrix} i_{c,a}^* \\ i_{c,b}^* \\ i_{c,c}^* \end{bmatrix} = \sqrt{\frac{2}{3}} \cdot \begin{bmatrix} \frac{1}{\sqrt{2}} & 1 & 0 \\ \frac{1}{\sqrt{2}} & -1 & \frac{\sqrt{3}}{2} \\ \frac{1}{\sqrt{2}} & -1 & -\frac{\sqrt{3}}{2} \end{bmatrix} \cdot \begin{bmatrix} -i_0 \\ i_{c,\alpha}^* \\ i_{c,\beta}^* \end{bmatrix}, \quad (9)$$

where \bar{p} is the DC component of the instantaneous power p , \tilde{p} is the AC component of the instantaneous power p , \tilde{p}_L is the AC component of the load active power, \bar{q} is the DC component of the instantaneous imaginary power q , \tilde{q} is the AC component of the instantaneous imaginary power q , \bar{q}_L is the DC component of the load imaginary power, \tilde{q}_L is the AC component of the load imaginary power, $i_{c,\alpha}^*$ is the reference signal of the SHAF in the (α) coordinate, $i_{c,\beta}^*$ is the reference signal of the SHAF in the (β) coordinate, $i_{c,a}^*$ is the reference signal of the SHAF in the (a) coordinate, $i_{c,b}^*$ is the reference signal of the SHAF in the (b) coordinate, and $i_{c,c}^*$ is the reference signal of the SHAF in the (c) coordinate.

Conventionally, to calculate the SEAF-required series injected voltage, the voltage phase angle is obtained using a phase locked loop (PLL), and then the V_{max} is multiplied by $\sin(\omega t)$ to get reference voltage (V_c) and the required injected voltage (V_{inj}) is calculated as follows [23]:

$$V_c = V_{max} \sin(\omega t), \quad (10)$$

$$V_{inj} = V_c - V_L, \quad (11)$$

where V_L is the actual load voltage and V_{inj} is the required injected series voltage.

3. Proposed fuzzy controlled EMS-connected UPQC

The proposed UPQC control is illustrated in the system as shown in Figure 1. The used system under study is configured with a substation transformer, PV farm, wind farm, linear load, and nonlinear load. The implementations of the proposed UPQC consist of three parts. The first one implements the fuzzy control system of the UPQC SHAF, the second part implements the fuzzy control system for the UPQC SEAF, and the third part implements the control system between the grid EMS and UPQC.

3.1. Proposed fuzzy controlled SHAF

The SHAF imposes a reversed harmonic effect to balance the load harmonics maintaining the supply current stable. To get sinusoidal current from the utility, the SHAF should supply harmonics current to the load. Also, it draws a real component of losses power from the supply to supply the switching losses and maintain the DC link voltage unchanged. The DC link capacitor mainly serves two purposes. First, it maintains a constant DC

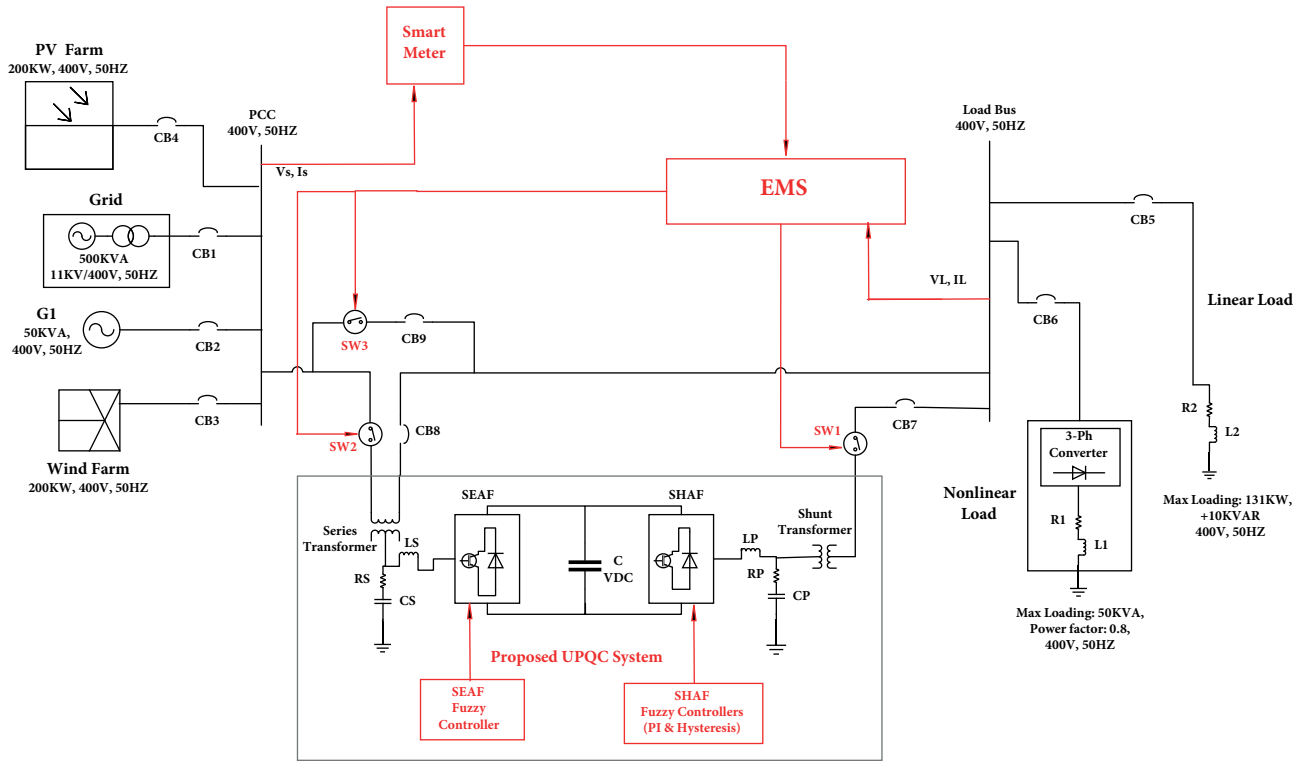


Figure 1. The configuration for used smart microgrid connected with the proposed UPQC system.

voltage, and also, it acts as an energy storage device to substitute the real power variance between load and grid source. The new proposed method of SHAF control configuration is completely based on fuzzy logic control, as shown in Figure 2.

The first fuzzy logic controller regulates the error between the DC link capacitor voltage and DC reference voltage. The output of the fuzzy logic controller gives the magnitude of the peak of source current (I_{max}) that compensates for DC link capacitor imbalance and switching losses of the SHAF. The PLL is used to get the source voltage phase angle. The obtained unit sine vectors in phase with the source voltage are multiplied by I_{max} to obtain the instantaneous source reference currents i_{sa}^* , i_{sb}^* , and i_{sc}^* . These source reference currents are compared respectively with the distorted source currents i_{sa} , i_{sb} , and i_{sc} . The error signals are sent to the second fuzzy logic controller in order to generate the switching firing pulses required for the SHAF inverter. The first fuzzy logic controller here is used to regulate the voltage across the DC bus capacitor to calculate I_{max} and it forms the control signal from the error signal (E) between capacitor voltage in the DC side and the reference DC voltage. The change in error (CE) is calculated as follows:

$$E(k) = V_{dcref} - V_{dc}, \quad (12)$$

$$CE = E(k) - E(k-1). \quad (13)$$

The first fuzzy logic controller has two input variables, (E) and (CE). Both of them have seven triangle membership functions (MF): LB (low big), LM (low medium), LS (low small), M (medium), HS (high small), HM (high medium), and HB (high big), as shown in Figures 3 and 4. The controller has one variable output

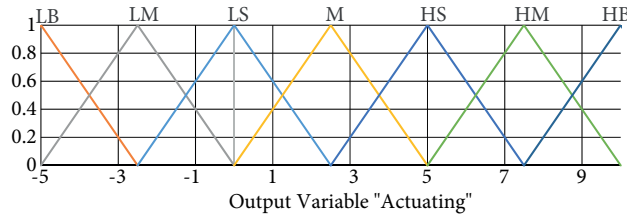


Figure 5. MFs for the output actuating signal I_{max} .

Table 1. SHAF fuzzy rules.

Error rate (CE)	Error (E)						
	LB	LM	LS	M	HS	HM	HB
LB	LB	LB	LB	LB	LM	LS	M
LM	LB	LB	LB	LM	LS	M	HS
LS	LB	LB	LM	LS	M	HS	HM
M	LB	LM	LS	M	HS	HM	HB
HS	LM	LS	M	HS	HM	HB	HB
HM	LS	M	HS	HM	HB	HB	HB
HB	M	HS	HM	HB	HB	HB	HB

between the reference and actual current is fed to the second fuzzy logic controller to get the firing pulses of the SHAF inverter. The second fuzzy controller has three input variables, e_1 (error of phase A), e_2 (error of phase B), and e_3 (error of phase C). They have two trapezoidal MFs named N (negative) and P (positive and equal zero), as shown in Figure 6. The controller has six outputs, P1 (firing pulses for SHAF inverter power electronic switch number 1), P2, P3, P4, P5, and P6. They have two triangle MFs, named Z (zero) and O (one), as shown in Figure 7. These firing signals are sent to the shunt active filter inverter’s six power electronic switches.

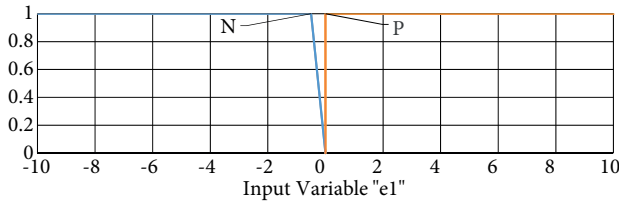


Figure 6. MFs for the input e_1 signal.

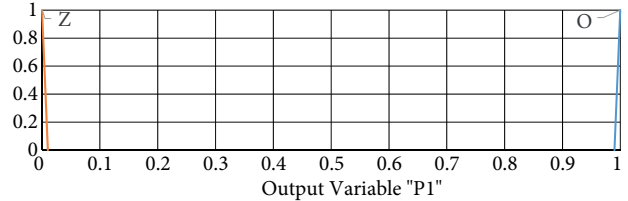


Figure 7. MFs for the output firing pulse signal P1.

3.1.2. Decision making of fuzzy firing control

In this stage and according to the required rule base function, input MFs correlate to the output MFs through the rules shown in Table 2. Centroid defuzzification is used and the crisp output is fed to the logic gate to change the crisp value of digital logic.

3.2. Proposed fuzzy controlled SEAF

The proposed SEAF compensates the grid voltage sag and voltage swell as it injects a compensating voltage so that the load voltage is perfectly balanced and is regulated. This paper illustrates a new method of SEAF control configuration using fuzzy logic control as shown in Figure 8.

Table 2. Second fuzzy rules.

e1	P1	P2	e2	P3	P4	e3	P5	P6
P	Z	O	P	Z	O	P	Z	O
N	O	Z	N	O	Z	N	O	Z

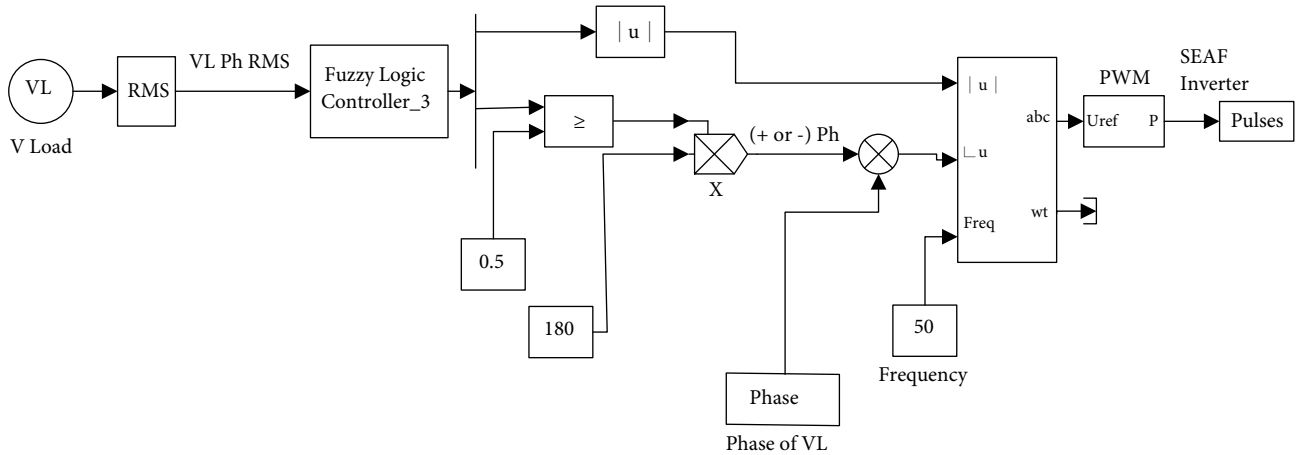


Figure 8. Block diagram of proposed fuzzy control system SEAF.

The load bus phase voltage RMS value is first measured by smart meter to trigger one of two cases: the first one if the load voltage is just below $(400/\sqrt{3})/\sqrt{2}V = (166V)$ and the second if the load voltage exceeds 166 V. The range of control is selected from 10% to 180% of nominal load voltage that gives from 16.6 V to 299 V with the accepted range from 95% to 105%. For either case, the crisp value of the load voltage triggers fuzzy values for seven triangle MFs named UB (under big) [16.6V: 61.4V], UM (under medium), [61.4V: 105.4V], US (under small) [104.4V: 157.7V], Accepted [157.7V: 174V], OB (over big) [262.6V: 299V], OM (over medium) [222.6V:262.6V], and OS (over small) [174V: 222.6V], as shown in Figure 9. When the first case is encountered, the SEAF will inject voltage in the phase of the grid voltage with required magnitude that will be controlled by reference signal amplitude (Ar) to change the inverter modulation index (Mi), where (Ac) is the amplitude of the carrier signal. Referring to the following equation, if $Ac = 1$, then $Mi = Ar$:

$$Mi = \frac{Ar}{Ac}. \tag{14}$$

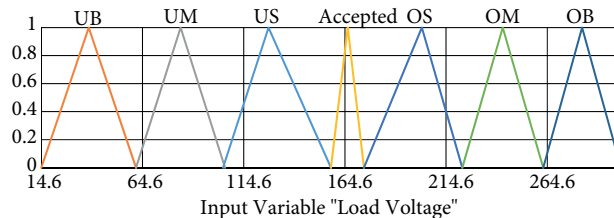


Figure 9. MFs for the load voltage input V_L .

When the second case is encountered, the SEAF will inject voltage opposite the grid voltage with appropriate modulation index. The fuzzy logic controller determines the reference signal amplitude to change the

modulation index for each case according to the severity of undervoltage or overvoltage with control resolution of [0.05 to 0.9]. The main voltage phase is measured by the smart meters. The proposed controller controls the positive sign and negative sign for the injected voltage by giving the output phase shift value (0° or 180°) to be added to the measured main voltage phase. If it equal to 0° that means the injected voltage is to be in phase with grid voltage in sag condition, and if it equals 180° that means the injected voltage is to be opposite the phase of the grid voltage in swell condition. The output crisp value of the amplitude reference Ar has four triangle MFs named L (low), M (medium), H (high), and Z (zero), as shown in Figure 10. The second output crisp value of the phase shift has two triangle MFs named Z (zero for 0°) and N (negative for 180°), as shown in Figure 11.

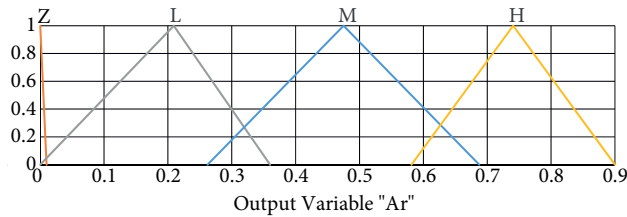


Figure 10. MFs for output reference signal Ar .

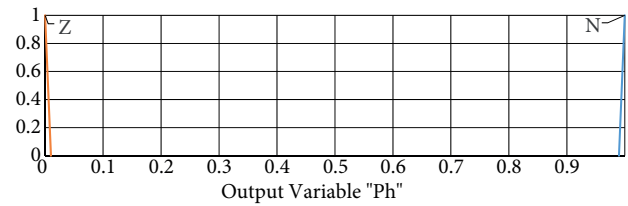


Figure 11. MFs for output phase shift.

3.2.1. Decision making of fuzzy voltage control

In this stage and according to the required rule base function, input MFs correlate to the output MFs as shown in Table 3.

Table 3. Fuzzy rules.

Load voltage	UB	UM	US	OB	OM	OS	Accepted
Ar	H	M	L	H	M	L	Z
Ph	Z	Z	Z	N	N	N	Z

3.3. Proposed EMS based UPQC control

The proposed control system in this part is applied with the smart microgrid EMS to control the UPQC SHAF and SEAF operations as shown in Figure 1. The EMS activates and deactivates the UPQC SHAF and SEAF to be in service in the required times only. First, the EMS controller receives the feedback from the grid for supplying current THD% at PCC, load voltages (RMS phase voltage), and DC capacitor voltage through smart meters. The EMS controller has three input variables of load voltage (V_L), $THD\%$, and capacitor charging status (V_{dc}). The input V_L has three variables: sag ($V_L < 95\%$), accepted (95% to 105%), and swell ($V_L > 105\%$). The second input $THD\%$ has two variables: accepted ($THD\% \leq 5\%$) and not accepted ($THD\% > 5\%$). The third input is the DC capacitor charging status (V_{dc}) and it has two variables: discharged and charged. The controller has three output digital variables, SW1, SW2, and SW3, to control the UPQC power electronic switches SW1, SW2, and SW3 according to the required process. Each output variable is either OFF (0) or ON (1). Figure 12 shows the flowchart of the control algorithm, including the decision-making of the EMS-based UPQC controller.

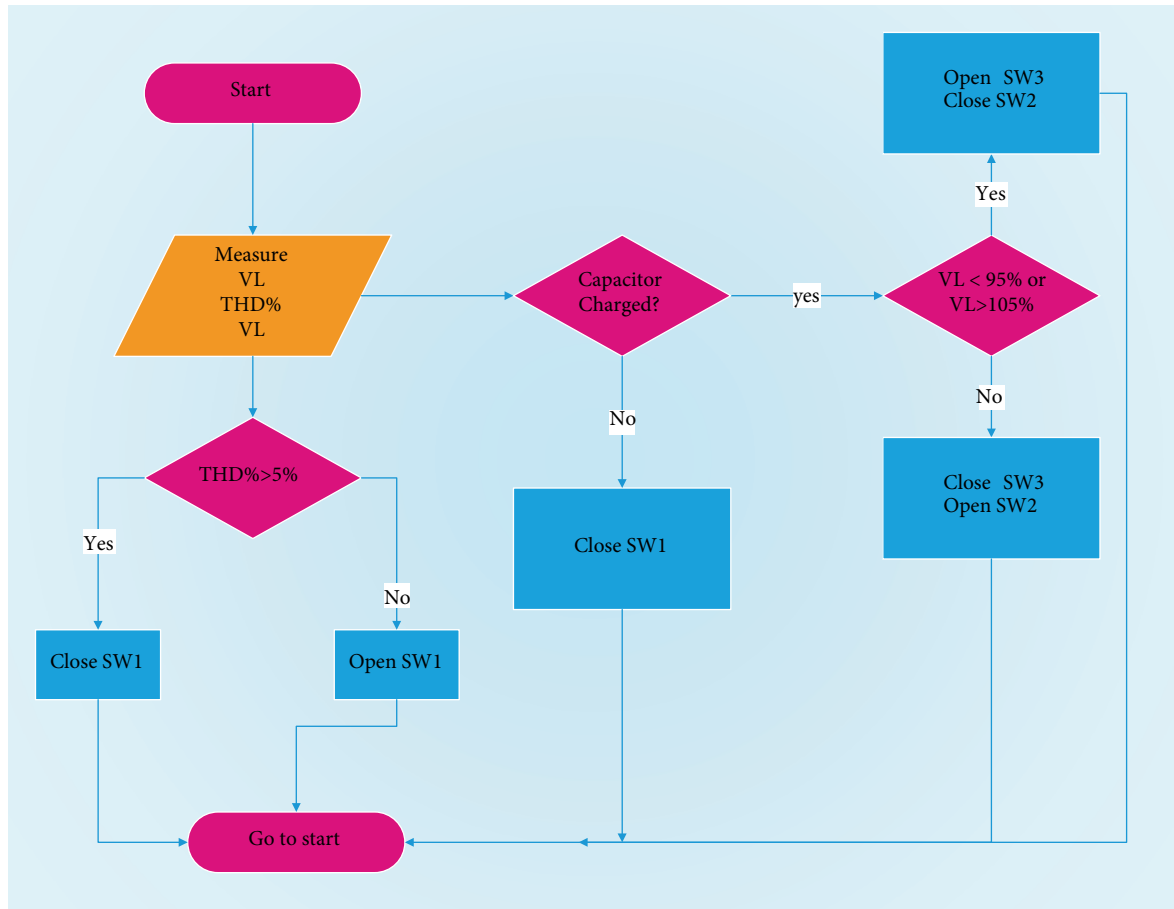


Figure 12. Flowchart for the proposed EMS-connected UPQC system.

4. The proposed system under study

The renewable generation data are based on [14]. The microgrid is supplied from the main grid through a 500 kVA substation transformer and the grid voltage is balanced at 400 V, 50 Hz. The microgrid contains one conventional three-phase 50 kVA diesel generator, a 200 kW wind farm, and a 200 kW PV plant. It is assumed that the conventional generator has both primary and secondary frequency control and that there is no damping or frequency dependent load. The wind farm and PV plants are assumed to be controlled by maximum power point tracking (MPPT). The maximum available power profiles for the wind farm and PV plant are obtained from [24, 25] as shown in Figure 13. Wind and PV plants operate at unity power factor and reactive power is only supplied from conventional generators and the grid. The assumed loads in the microgrid are of three types (active power linear load, inductive reactive power linear load, and nonlinear load), as shown in Figure 14. Table 4 shows the odd harmonic characteristics for the proposed nonlinear load. The proposed 50.4 kVA nonlinear load consists of a three-phase rectifier with third harmonic current injection. The characteristics of the nonlinear load are shown in Table 4.

5. Results and discussion

The smart microgrid system is studied for 24 h with varying linear and nonlinear load profiles and varying renewable energy generation of solar and wind energy. The supply current total harmonic distortion is evaluated

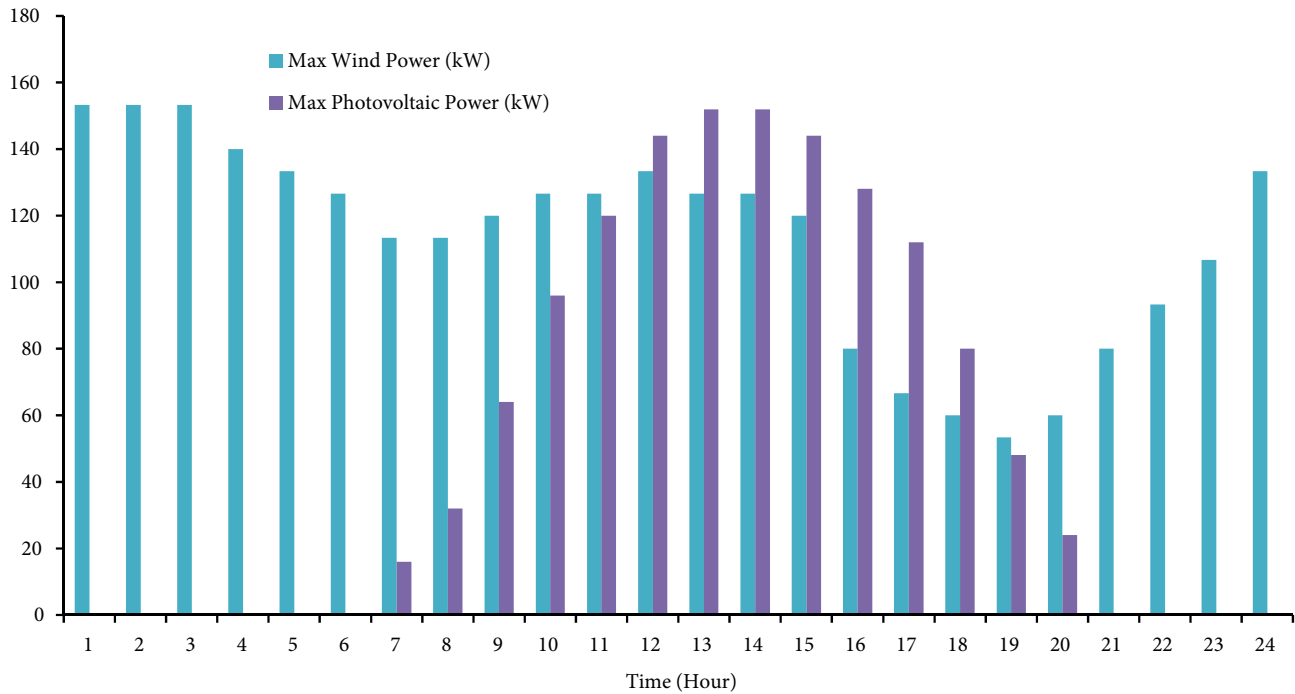


Figure 13. Maximum wind and PV power generations for a day for proposed smart microgrid system [14].

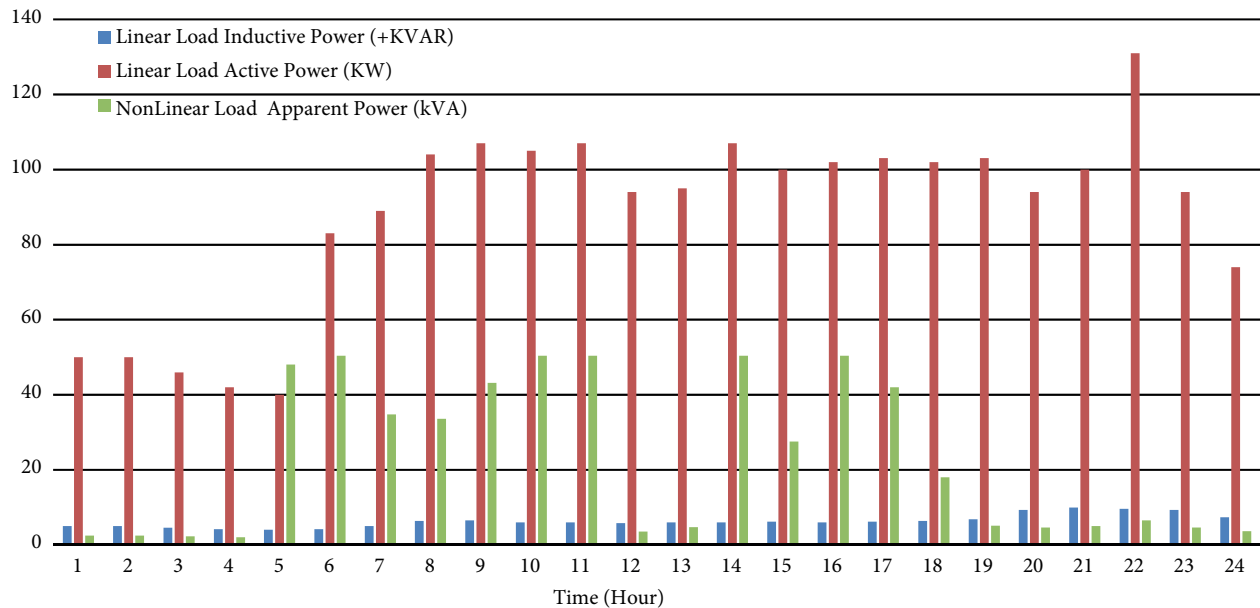


Figure 14. Proposed linear load and nonlinear load profiles for a day for proposed smart microgrid system.

at the point of common coupling (PCC) each hour. Evaluation of current harmonic distortion is performed using a fast Fourier transform (FFT). Voltage sag of 15% is assumed to occur in the eleventh hour. Voltage swell of 15% is assumed to occur in the fourth hour. The smart microgrid under study is simulated using MATLAB/Simulink with sample time of 5×10^{-6} and the UPQC is proposed to be in service after 0.02 s. The simulation results are given as follows.

Table 4. Odd harmonics characteristics of proposed nonlinear load.

	DC component	Fund.	(h3)	(h5)	(h7)	(h9)	(h11)	(h13)	(h15)	(h17)	(h19)
% of Fundamental	0.48%	100%	5.65%	22.30%	10.92%	0.29%	8.32%	6.15%	0.43%	7.70%	4.06%
Phase degree	90	-32.6	-58.5	170.5	173.4	232.1	-16.3	-12.7	35.5	157	162.9

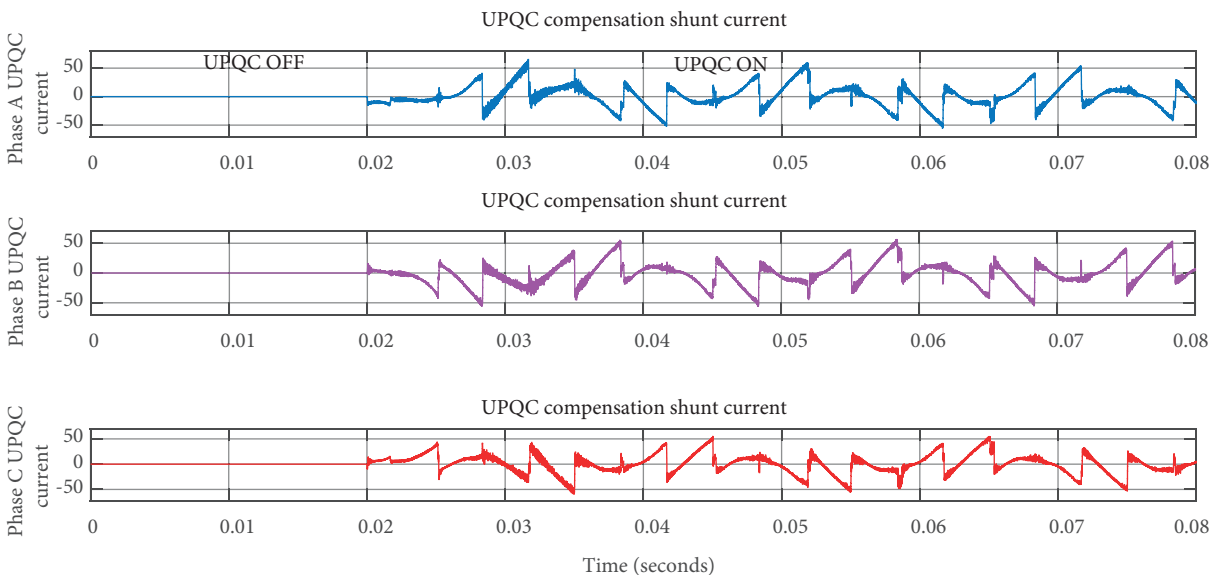
5.1. Harmonics evaluation and mitigation

The percentage THD of the supply current (equal to the total load current before UPQC activation) is measured each hour as shown in Table 5. The THD% of the supply current is exceeding the standards' limit of 5% for 9 h of the 24 h in a day. The maximum THD% is at the fifth hour with a value of 13.13%. The nonlinear load at this hour is about 52% of the total connected load. From the analysis of the microgrid harmonics during 24 h, as shown in Table 5, the total harmonics distortion of the supply current is more than 5% at the working hours of 5, 6, 7, 9, 10, 11, 14, 16, and 17. Therefore, the EMS activates the proposed UPQC SHAF to mitigate the harmonics at these times. All results for THD% after mitigation are shown in Table 5. Analyzing the harmonics spectrum during the fifth hour before connecting the SHAF, the THD% was 13.13%, but after using the proposed SHAF, the THD% is reduced to 4.9%. Figure 15 shows the UPQC shunt current compensation waveform at the PCC at the fifth hour. Figure 16 shows the waveforms of the load current and the supply current at the fifth hour with and without the proposed UPQC.

5.2. Voltage sag and swell

5.2.1. Voltage sag

At the eleventh hour (the time of peak loads), the loads are exposed to grid voltage sag of 15% of rated voltage. Using the proposed UPQC SEAF, the load voltage is not affected by the grid voltage sag and is still stable

**Figure 15.** UPQC shunt current compensation at PCC at fifth hour.

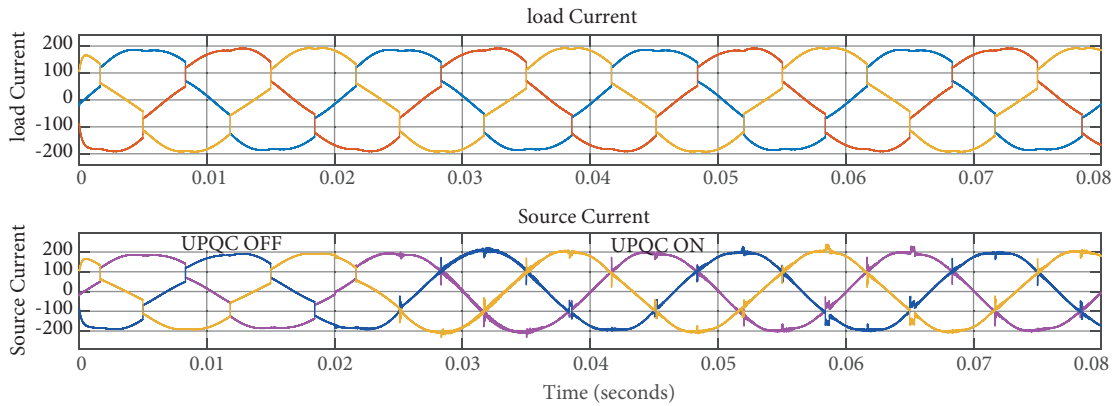


Figure 16. Load current and supply current waveforms at fifth hour.

Table 5. Total harmonics distortion at PCC for 24 h.

Time (H)	THD% without UPQC	THD% with UPQC	EMS control SHAF (SW1)	Time (H)	THD% without UPQC	THD% with UPQC	EMS control SHAF (SW1)
1	0.89%	NA	Deactivated	13	0.90%	NA	Deactivated
2	0.89%	NA	Deactivated	14	6.84%	2.26%	Activated
3	0.89%	NA	Deactivated	15	4.38%	NA	Deactivated
4	0.90%	NA	Deactivated	16	7.10%	2.32%	Activated
5	13.13%	4.90%	Activated	17	6.06%	2.01%	Activated
6	8.28%	2.69%	Activated	18	2.93%	NA	Deactivated
7	5.85%	1.96%	Activated	19	0.89%	NA	Deactivated
8	4.98%	NA	Deactivated	20	0.89%	NA	Deactivated
9	6.03%	2%	Activated	21	0.89%	NA	Deactivated
10	6.94%	2.29%	Activated	22	0.89%	NA	Deactivated
11	6.84%	2.24%	Activated	23	0.89%	NA	Deactivated
12	0.69%	NA	Deactivated	24	0.89%	NA	Deactivated

with full rated voltage as shown in Figure 17, which shows the RMS phase voltage of the grid and load voltages during the voltage sag period.

5.2.2. Voltage swell

At the fourth hour (the time of lowest load value), the loads are exposed to grid voltage swell of 15% of rated voltage. Using the proposed UPQC SEAF, the load voltage is not affected by the grid voltage swell and is still stable with full rated voltage as shown in Figure 18, which shows the RMS phase voltage of the grid and load voltages during the voltage swell period.

5.3. UPQC activation and deactivation duty

The UPQC SEAF is activated only at the fourth and eleventh hours by the EMS, which needs the charging process of the DC capacitor to be activated by the SHAF. Referring to Table 5, it is obvious that the UPQC SHAF is activated also by the EMS at the eleventh hour to guarantee the capacitor charging process. At the

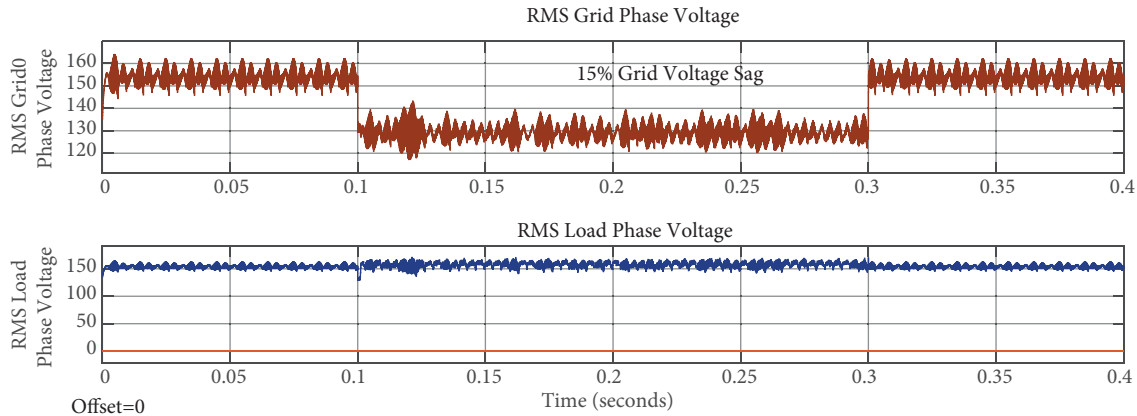


Figure 17. Grid and load RMS phase voltages at eleventh hour before and after using UPQC.

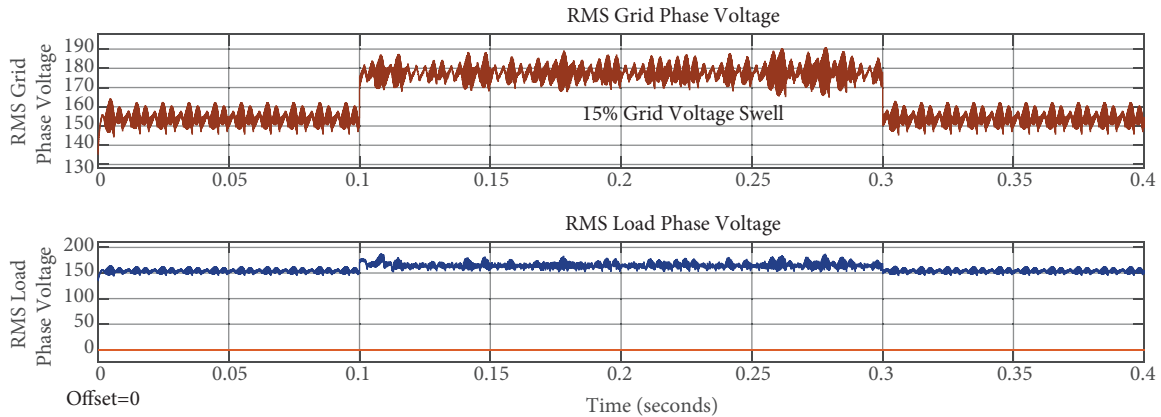


Figure 18. Grid and load RMS phase voltages at fourth hour before and after using UPQC.

fourth hour, there is no need for the SHAF as the percentage THD is accepted at this time. The EMS will control the capacitor charging process at this hour to activate the SHAF at the fourth hour to charge the capacitor for SEAF function only. In total, the UPQC is activated for 10 h (at times of 4, 5, 6, 7, 9, 10, 11, 14, 16, and 17) and it is deactivated for 14 h. As shown in Figure 19 the UPQC is activated only for 42% of the day's hours. This means it will be at rest for 58% of the day's hours, contrary to previous works, which considered the UPQC to be connected continuously to the grid. Figure 19 shows the activation and deactivation duty of the proposed EMS-controlled UPQC considering the change in percentage THD and the grid voltage throughout the day's cycle with proposed sample time (1 ms). This approach adds the following benefits:

- The probability of exposing the UPQC to grid faults is decreased to be 42%.
- The UPQC is mainly built using power electronic switches that generate high amounts of heat and need continuous cooling, so the proposed approach reduces thermal stresses on the UPQC components.
- Consequently, it increases the lifetime of the UPQC.

5.4. Compared to the conventional UPQC control methods

Conventional techniques published so far in the literature have a greater computational burden and also most of them use P-Q instantaneous theory [19], which makes these techniques more complicated. The proposed method is a simple approach for effective current harmonics compensation and voltage sags and swells compensation.

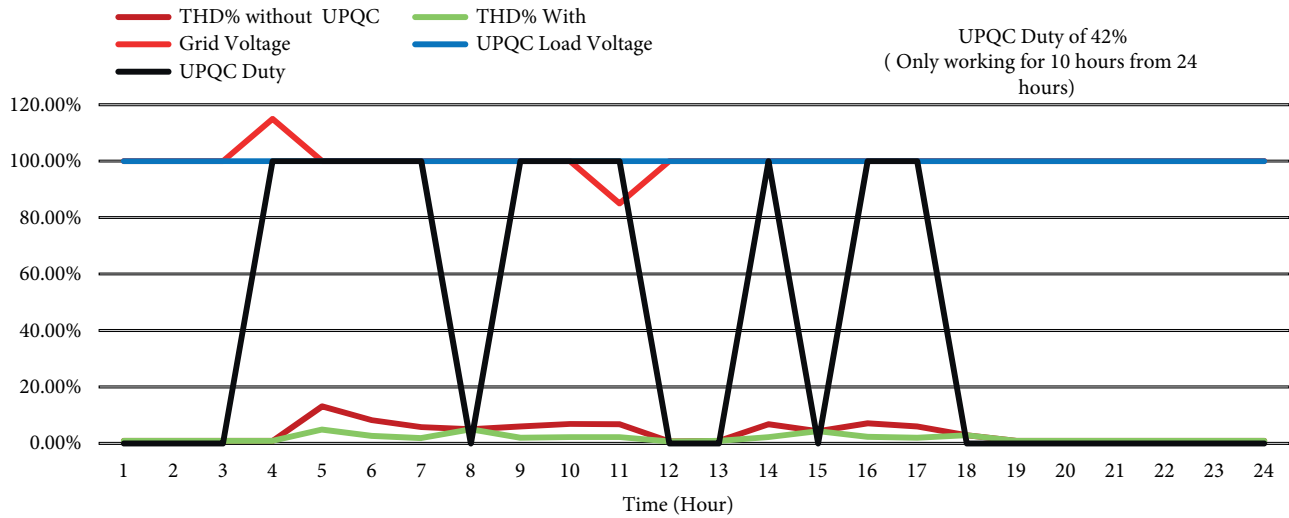


Figure 19. UPQC duty considering the change in percentage THD and the grid voltage.

In order to compare the proposed approach with the conventional P-Q method [19] and the literature's fuzzy controlled UPQC [20, 21], each method is simulated on the system under study at the fifth hour and sixth hour. The total harmonic distortion at the PCC without UPQC and with UPQC is measured. The results obtained from all of these techniques are compared in Table 6. The simulation results verify the good performance for the proposed UPQC introduced in this work in harmonic mitigation. The voltage source is subjected to voltage sag of 15% and the simulation results obtained by using conventional and fuzzy UPQC successfully address

Table 6. Comparative study between proposed UPQC and literatures.

Comparison item	P-Q-based UPQC	Literature's fuzzy UPQC	Proposed fuzzy UPQC
UPQC shunt part reference signal generation	PI controller, Clark's transformation, PQ calculation	Fuzzy controller, Clark's transformation, PQ calculation	Completely fuzzy controlled
Shunt part inverter firing signal generation	Hysteresis controller	Hysteresis controller	Fuzzy controller
Series part reference signal generation	Mathematical calculation	Mathematical calculation	Fuzzy controller
Series part inverter firing signal generation	PWM hysteresis controller	PWM hysteresis controller	Fuzzy control with PWM
Classical mathematical models need	Depends on mathematical model	Depends on mathematical model	No need for accurate mathematical model
Complexity of design	Complex	Complex	Simple
THD% at fifth hour	6.2%	4.98%	4.9%
THD% at sixth hour	4.1%	2.87%	2.69%
Load voltage during 15% grid voltage sag	99%	99%	100%
UPQC duty control	N/A	N/A	EMS controlled
UPQC duty	100%	100%	42%

the voltage sag problem. However, the proposed UPQC is based on a simpler fuzzy control. Table 6 gives a comparative study between the literature's P-Q UPQC [19], the literature's fuzzy controlled UPQC [20, 21], and the proposed fuzzy UPQC in this work.

6. Conclusions

This paper illustrates a new method for a UPQC control system based on fuzzy logic control, which is simple and robust. Analyzing the simulation results for the proposed smart microgrid system shows that after activating the proposed UPQC the percentage THD values are reduced below 5% to become well within the acceptable range with a maximum value of 4.9% at the fifth hour. The results showed the effectiveness of the proposed UPQC control in compensating voltage sag and swell. In conclusion, the proposed system succeeds in solving the power quality problems of harmonics, voltage sag, and voltage swell for smart microgrids considering the variation of renewable energy supply and the variation of loads throughout the day's cycle. The proposed system is fully controlled through the smart microgrid's EMS to be activated automatically during disturbance times only. That activates the UPQC to be connected to the grid only for 42% of the day's hours, contrary to previous work, and this improves the UPQC lifetime.

References

- [1] Potocnik J. Definition adapted from the European Technology Platform Smart Grid (ETPSG). Brussels, Belgium: European Communities, 2006.
- [2] IEEE. Std 519-2014, IEEE Recommended Practice and Requirements for Harmonic Control in Electric Power Systems. New York, NY, USA: IEEE Standards, 2014.
- [3] IEEE. Std 1159-2009, IEEE Recommended Practice for Monitoring Electric Power Quality. New York, NY, USA: IEEE Standards, 2009.
- [4] IEEE. Std 1547-2018, IEEE Standard for Interconnection and Interoperability of Distributed Energy Resources with Associated Electric Power Systems Interfaces. New York, NY, USA: IEEE Standards, 2018.
- [5] Kuzlu M, Pipattanasomporn M, Rahman S. A comprehensive review of smart grid related standards and protocols. In: IEEE 2017 International Conference of Smart Grid and Cities Congress and Fair; İstanbul, Turkey; 2017. pp. 12-16.
- [6] Peng FZ. Flexible AC transmission systems (FACTS) and resilient AC distribution systems (RACDS) in smart grid. *Proceedings of the IEEE* 2017; 105 (11): 2099-2115. doi: 10.1109/JPROC.2017.2714022
- [7] Amaripadath D, Roche R, Joseph-Auguste L, Istrate D, Fortune D et al. Power quality disturbances on smart grids: overview and grid measurement configurations. In: IEEE 2017 Universities Power Engineering Conference; Heraklion, Greece; 2017. pp. 1-6.
- [8] Yoldaş Y, Önen A, Muyeen SM, Vasilakos AV, Alan İ. Enhancing smart grid with microgrids: challenges and opportunities. *Renewable and Sustainable Energy Reviews* 2017; 72 (1): 205-214. doi: 10.1016/j.rser.2017.01.064
- [9] Bollen MH, Das R, Djokic S, Ciufu P, Meyer J et al. Power quality concerns in implementing smart distribution-grid applications. *IEEE Transactions on Smart Grid* 2016; 8 (1): 391-399. doi: 10.1109/TSG.2016.2596788
- [10] Zhengyou M, Deyang S. Study on the application of advanced power electronics in smart grid. In: IEEE 2017 Sixth International Conference on Future Generation Communication Technologies; Dublin, Ireland; 2017. pp. 96-99.
- [11] Moghbel M, Masoum MA, Fereidouni A, Deilami S. Optimal sizing, siting and operation of custom power devices with STATCOM and APLC functions for real-time reactive power and network voltage quality control of smart grid. *IEEE Transactions on Smart Grid* 2018; 9 (6): 5564-5575. doi: 10.1109/TSG.2017.2690681

- [12] Gandoman FH, Ahmadi A, Sharaf AM, Siano P, Pou J et al. Review of FACTS technologies and applications for power quality in smart grids with renewable energy systems. *Renewable and Sustainable Energy Reviews* 2018; 82 (1): 502-514. doi: :10.1016/j.rser.2017.09.062
- [13] Khorasani PG, Joorabian M, Seifossadat SG. Smart grid realization with introducing unified power quality conditioner integrated with DC microgrid. *Electric Power Systems Research* 2017; 151 (1): 68–85. doi: 10.1016/j.epsr.2017.05.023
- [14] Youssef KH. Power quality constrained optimal management of unbalanced smart microgrids during scheduled multiple transitions between grid-connected and islanded modes. *IEEE Transactions on Smart Grid* 2017; 8 (1): 457–464. doi: 10.1109/TSG.2016.2577643
- [15] Hafezi H, Faranda R. Open UPQC series and shunt units cooperation within smart LV grid. In: *IEEE 2017 International Conference of Clean Electrical Power*; Santa Margherita Ligure, Italy; 2017. pp. 304-310.
- [16] Ceaki O, Seritan G, Vatu R, Mancasi M. Analysis of power quality improvement in smart grids. In: *IEEE 2017 The 10th International Symposium on Advanced Topics in Electrical Engineering*; Bucharest, Romania; 2017. pp. 797-801.
- [17] Gheorghe S, Golovanov N, Lazaroïu GC, Porumb R. Smart grid, integration of renewable sources and improvement of power quality. In: *IEEE 2017 21st International Conference on Control Systems and Computer Science*; Bucharest, Romania; 2017. pp. 641-645.
- [18] Hafezi H, D'Antona G, Dedè A, Giustina DD, Faranda R et al. Power quality conditioning in LV distribution networks: results by field demonstration. *IEEE Transactions on Smart Grid* 2017; 8 (1): 418 – 427. doi: 10.1109/TSG.2016.2578464
- [19] Jadhao SS, Ratnaparkhi GP, Dhole GM, Paraskar SR. Voltage quality enhancement using unified power quality conditioner (UPQC). In: *IEEE 2017 International Conference on Energy, Communication, Data Analytic and Soft Computing*; Chennai, India; 2017. pp. 3270-3274.
- [20] Almelian MM, Mohd II, Omran MA, Sheikh UU. Performance of unified power quality conditioner (UPQC) based on fuzzy controller for attenuating of voltage and current harmonics. In: *IOP 2018 International Conference on Innovative Technology, Engineering and Sciences*; Pekan, Malaysia; 2018. pp. 1-11.
- [21] Benachaïba C, Haidar AM, Habab M, Abdelkhalek O. Smart control of UPCQ within microgrid energy system. *Energy Procedia* 2011; 6 (1): 503–512. doi: 10.1016/j.egypro.2011.05.058
- [22] Morán L, Dixon J, Rashid MH. *Active Filters: Power Electronics Handbook*. Burlington, MA, USA: Elsevier Press, 2011.
- [23] Kumar AS, Rajasekar S, Raji PA. Power quality profile enhancement of utility connected microgrid system using ANFIS-UPQC. *Procedia Technology* 2015; 21 (1): 112 – 119. doi: 10.1016/j.protcy.2015.10.017
- [24] Homae O, Zakariazadeh A, Jadid S. Real time voltage control algorithm with switched capacitors in smart distribution system in presence of renewable generations. *Electrical Power and Energy Systems* 2014; 54 (1): 187-197. doi:10.1016/j.ijepes.2013.07.010
- [25] Christakou K, Tomozei DC, Bahramipناه M, Le Boudec JY, Paolone M. Primary voltage control in active distribution networks via broadcast signals: the case of distributed storage. *IEEE Transactions on Smart Grid* 2014; 5 (5): 2314-2325. doi: 10.1109/TSG.2014.2319303